

# A guide to establishing hollow fiber macroscopic properties for membrane applications

Scott A. McKelvey, Dominic T. Clausi, William J. Koros \*

*Department of Chemical Engineering, University of Texas at Austin, Austin, TX 78712-1062, USA*

Received 18 December 1995; revised 12 August 1996; accepted 12 August 1996

---

## Abstract

Production of advanced hollow fiber membranes involves optimizing permeation and mechanical properties. If mechanical properties are insufficient, time dependent losses in permeation performance will occur. Practically speaking, *numerous* hollow fiber properties are considered and established concurrently; however, such a discussion would be quite complex for a single manuscript. Therefore, this work focuses on the specification and establishment of large-scale *macroscopic* properties such as those identified in Table 1. With *optimal* macroscopic properties specified, a basic understanding of fiber spinning couples process variables and macroscopic properties. This paper focuses on *dry-jet* wet spinning and associated processing complications, since these complications represent the first practical hurdles that must be overcome to produce useful continuous fiber suitable for membrane applications.

**Keywords:** Asymmetric hollow fibers; Dry-jet wet spinning; Gas separation; Mechanical integrity

---

## 1. Introduction

The first mention of hollow fiber membranes appears to be in a series of patents by Mahon in 1966 assigned to the Dow Chemical Company [1,2]. Polymeric hollow fibers for membrane applications are formed by extruding a polymer solution through an annular aperture in a device called a spinneret. Extrudate is prevented from collapsing by coextruding a liquid or a gas in the center of the annulus to form the hollow region, commonly called the fiber *bore* or *lumen* (see Fig. 1).

The extrudate is accelerated to a higher velocity by applying an external force. This external force

can be only gravity but commonly the dominant external force is provided by a *godet* or a *take-up drum*. The process of accelerating the extrudate or *filament* is called *drawing*, the path that the filament takes is referred to as the *spin line*, and the complete process is referred to as *fiber spinning* (see Fig. 2a).

Generally, polymer cannot be processed as a melt to form acceptable morphologies for membrane applications, so a polymer solution, commonly called *dope*, must be extruded. Dope is extruded and vitrification occurs as a result of mass and/or heat transfer. The overall process of converting a polymer solution to a high-performance hollow fiber membrane is extremely complex and entails highly sophisticated mechanical, thermodynamic, and kinetic considerations. If the spin line is only exposed to a gaseous environment prior to vitrification, the pro-

---

\* Corresponding author.

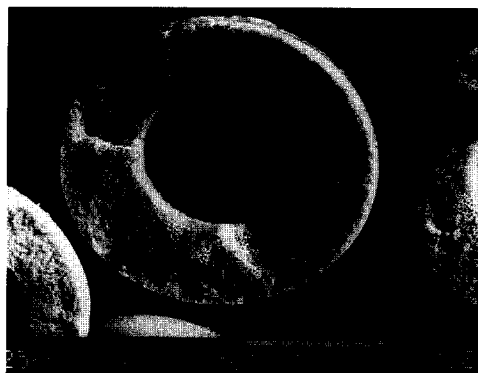


Fig. 1. Scanning electron photomicrograph of a typical polysulfone hollow fiber with 'optimal' macroscopic properties. Note the hollow dark center region which is called the bore or lumen. The fiber outside and inside diameters were approximately 200 and 100  $\mu\text{m}$ , respectively. Fiber spun from 40% PSF Udel® 1835, 36% DMAC, 12% THF, and 12% EtOH. Dope flow rate 180 cc/h, bore fluid (90% NMP in water) flow rate 20 cc/h, take-up rate 80 m/min, and gap height 2 cm. Spinneret temperature 25°C and quench temperature 8°C. Spinneret diameters:  $D_1/D_2/D_3 = 0.8/0.4/0.2$  mm.

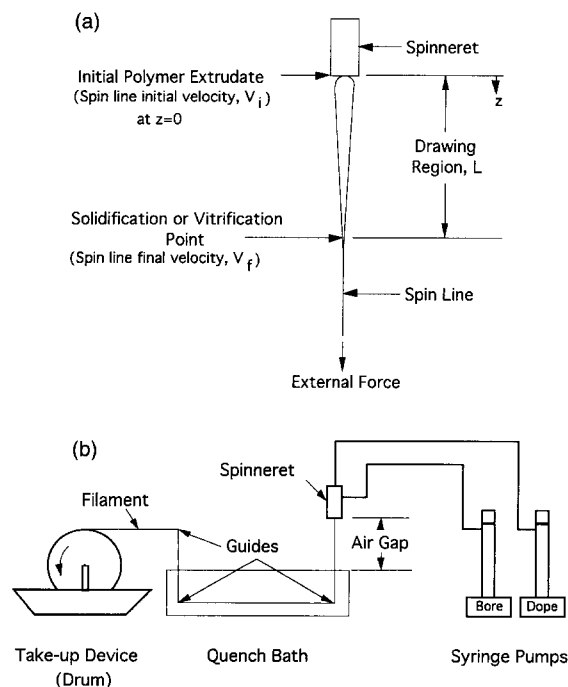


Fig. 2. (a) Schematic of general fiber spinning process. (b) Schematic of dry-jet fiber spinning process.

cess is called dry-jet spinning. If the spin line is only exposed to a liquid environment prior to vitrification, the process is called *wet-jet* spinning. Whenever vitrification occurs quickly the process is referred to as *quenching*, this is often the case during wet-jet spinning.

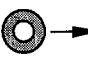
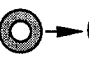


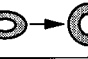
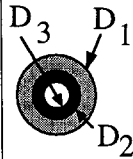
To obtain small diameter hollow fiber (i.e. < 500  $\mu\text{m}$ ), the spin line must be drawn due to practical limitations in fabricating spinnerets with small orifices. Dry-jet spinning offers the advantageous ability to draw the spinning line to very small diameters since vitrification often occurs slowly relative to wet-jet spinning. Small diameter fiber is formed using high draw ratios (typically 5–15 although draw ratios may be even higher), which may be associated with high tensile stress on the spin line (typically measured tensile force is about 1–5 cN). Small diameter fiber may only be spun continuously if the fiber is able to accommodate these tensile loads without breaking the spin line. In some cases, high draw ratios can result in increased chain orientation, which may or may not be advantageous for a desired membrane application [3].

When quick vitrification and small diameters are desired, as in the production of most gas separation membranes, drawing may occur in a gaseous environment (*air gap*) prior to quenching in a liquid nonsolvent bath. The distance between the spinneret face and the quench bath is called the gap height. This hybrid process is called dry-jet wet spinning (see Fig. 2b). Moreover, the possible benefit of exposing the nascent membrane to an environment drastically different than the quench bath prior to quenching is appealing and can aid in the formation of highly asymmetric structures. The first environment hypothetically initiates the formation of the permselective skin and the quench environment completes the formation of the permselective skin and the formation of the porous substrate. These concepts regarding the development of highly asymmetric structures are extensions of the pioneering work by Loeb and Sourirajan [4]. Many others have been influential in this active research area [5–10].

This paper focuses on dry-jet wet spinning, since it appears to be the most flexible and widely practiced method of hollow fiber membrane formation, especially for gas separation applications. The aim of this paper is to describe the effects of primary pro-

Table 1

A preliminary guide to controlling several macroscopic properties using dominant process variables. Shaded blocks identify dominant process variables controlling a given macroscopic property. For example,  $\langle OD \rangle$  is primarily controlled by manipulating draw ratio, DR. Terms and symbols are explained in accompanying text

Macroscopic Properties							
	$\langle OD \rangle$	$\langle ID \rangle$	Diameter Variance, DV	Non-Concentric Bores, NCB	Irregular Bores, IB	Ovality, OV	Fiber Breaks, FB
							
Processing Parameters	 Spinneret Design, SD	Second-order to DR.	Second-order to $Q_b$ .		Verify concentricity of $D_1, D_2, D_3$ . Can require new SD to improve dope flow axisymmetry.		SD often limits maximum $Q_d$ due to dope elasticity and excessive pressure drop across spinneret.
	Dope Extrusion Rate, $Q_d$	$\langle OD \rangle$ decreases as $Q_d$ decreases when take-up velocity is held constant.					FB increase as $Q_d$ increases when DR is held constant due to dope elasticity. Elastic effects often limit production rates.
	Draw Ratio, DR $\frac{V_f}{\langle V_i \rangle}$	$\langle OD \rangle$ decreases as DR increases.	$\langle ID \rangle$ is controlled by $Q_b$ once $\langle OD \rangle$ is established using DR and $Q_d$ .	Highly dope specific; however, DV often decreases as DR decreases.	Second-order to SC; however, IB tend to decrease as DR decreases.	Second-order to location of SLG; however, OV tends to decrease as DR increases since decreasing $\langle OD \rangle$ increases VK.	Typically, FB decrease as DR decreases since tensile stress tends to be reduced.
	Gap Height, GH			DV dependent on GH but highly dope specific.	Second-order to SC.	Second-order to VK in quench bath.	FB dependent on GH but highly dope specific.
	Bore Fluid Extrusion Rate, $Q_b$	Second-order to DR.	$\langle ID \rangle$ decreases as $Q_b$ decreases.			Second-order to location of SLG; however, OV tends to decrease as $Q_b$ increases since increasing $\langle OD \rangle / \langle ID \rangle$ increases VK.	
	Solvent Concentration in Bore Fluid, SC				IB decrease as SC increases.	OV tends to decrease as SC decreases since SC is coupled to VK.	Low SC can increase FB.
	Vitrification Kinetics, VK	Fiber shrinkage is second-order to DR.	Second-order to $Q_b$ .	Highly dope specific; however, DV tends to decrease as VK increase (i.e., dampens instabilities).	IB decrease as VK at fiber $\langle ID \rangle$ decrease (e.g., increase SC).	OV decreases as VK increases.	Highly dope specific; however, decreasing VK often allows increased drawing without FB.
	Spin Line Guides, SLG			Minimize fluctuations in tensile force (e.g., variations in SLG friction).		OV decreases as residence time in quench bath before contacting first SLG increases.	Decrease FB in or after the quench bath by decreasing SLG friction.

cess variables controlling the fiber properties identified across the top of Table 1. Because of the large-scale of these properties relative to other morphological features essential for efficient separation of gases, these properties can be termed ‘macroscopic.’ The primary processing (i.e., spinning) parameters influencing these properties are listed along the left hand side of Table 1. Many complications can be encountered during fiber spinning. This paper and an accompanying appendix, Appendix A, highlight key problems and their possible solutions.

## 2. Optimal macroscopic properties

Increasing membrane surface area in a given module volume is a common approach to increase module productivity. Therefore, smaller diameter fibers are favored and typical average outside fiber diameters,  $\langle OD \rangle$ , range from 600 to 100  $\mu\text{m}$  in gas separation applications. Average inside fiber diameter,  $\langle ID \rangle$ , is limited by gas pressure drop down the fiber bore, since pressure drop is inversely proportional to  $\langle ID \rangle$  to the fourth power. In practical applications, pressure drop becomes severe at  $\langle ID \rangle$ 's less than 50  $\mu\text{m}$ . Minimum fiber  $\langle OD \rangle$  is therefore



Fig. 3. Macroscopic fiber failure due to an internally fed pressure difference of 550 psid. The fiber  $\langle OD \rangle$  and  $\langle ID \rangle$  were approximately 800 and 400  $\mu\text{m}$ , respectively. Fiber spun from 40% PSF Udel® 1800, 36% DMAC, 12% THF, and 12% EtOH. Dope flow rate 150 cc/h, bore fluid (50% potassium acetate in water) flow rate 60 cc/h, and take-up rate 7.5 m/min based on Pesek [15]. Spinneret temperature was room temperature but uncontrolled. Spinneret diameters:  $D_1 / D_2 / D_3 = 0.9/0.4/0.2$  mm.

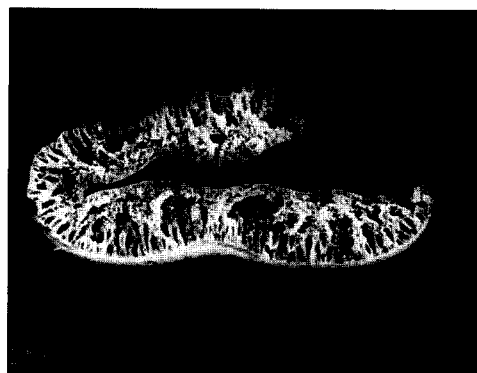


Fig. 4. Macroscopic fiber failure due to an externally fed pressure difference of 500 psid. The fiber  $\langle OD \rangle$  and  $\langle ID \rangle$  diameters were approximately 800 and 400  $\mu\text{m}$ , respectively. Fiber spun from 40% PSF Udel® 1800, 36% DMAC, 12% THF, and 12% EtOH. Dope flow rate 150 cc/h, bore fluid (50% potassium acetate in water) flow rate 60 cc/h, and take-up rate 7.5 m/min based on Pesek [15]. Spinneret temperature was room temperature but uncontrolled. Spinneret diameters:  $D_1 / D_2 / D_3 = 0.9/0.4/0.2$  mm.

determined by the wall thickness required to provide mechanical support.

One published ‘rule-of-thumb’ regarding wall thickness is based on the work of Ekiner and Vassilatos [11] implying a value of 2 for the  $\langle OD \rangle / \langle ID \rangle$  ratio. In our experience, this appears to be a reason-



Fig. 5. Scanning electron photomicrograph cross-section of a polysulfone hollow fiber with an irregular bore. Fiber spun from 40% PSF Udel® 1800, 36% DMAC, 12% THF, and 12% EtOH. Dope flow rate 150 cc/h, bore fluid (55% potassium acetate in water) flow rate 60 cc/h, and take-up rate 7.5 m/min based on Pesek [15]. Spinneret temperature was room temperature but uncontrolled. Spinneret diameters:  $D_1 / D_2 / D_3 = 0.9/0.4/0.2$  mm.

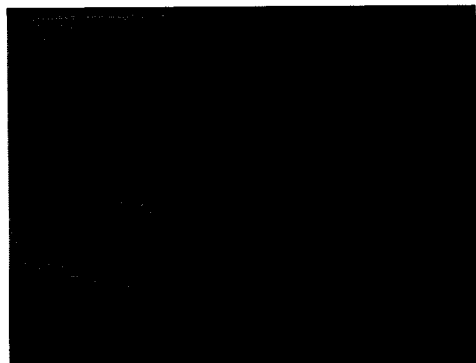


Fig. 6. Scanning electron photomicrograph of a fiber cross-section with an oval bore. Fiber spun from 24% Matrimid® 5292, 18% isobutanol, 55% NMP, and 3% 1,4-dioxane. Dope flow rate 180 cc/h, bore fluid (85% NMP in water) flow rate 50 cc/h, and take-up rate 80 m/min. Spinneret temperature 65°C and quench temperature 28°C. Spinneret diameters:  $D_1/D_2/D_3 = 0.9/0.4/0.2$  mm.

able practical value; however, mechanical integrity currently can be determined only empirically due to the complexity of an appropriate stress analysis [12]. If the mechanical integrity is insufficient, macroscopic fiber failure can result as shown in Figs. 3 and 4.

Several other macroscopic features jeopardize mechanical integrity and should be minimized. Some examples include irregular bores, nonconcentric bores, and oval fibers. Examples of irregular bores and oval fibers are shown in Figs. 5 and 6.

Fiber diameter variability also affects mechanical integrity. Moreover, high variances in  $\langle OD \rangle$  mag-



Fig. 7. Cross-sections of fiber cut from a single continuous spin line.

nify uncertainty in estimating membrane surface area and high variances in  $\langle ID \rangle$  induce variations in the pressure drop down the fiber bore. An example of variability in potted fiber  $\langle OD \rangle$  is shown in Fig. 7.

Considering these issues, a general 'optimal' starting point for gas separation hollow fiber macroscopic properties is a fiber  $\langle OD \rangle$  near 200  $\mu\text{m}$ ,  $\langle ID \rangle$  near 100  $\mu\text{m}$ , and low variance in both diameters. Of course, the 'optimal' dimensions and tolerances will vary depending on the specific application. An example of fiber with 'optimal' macroscopic properties is shown in Fig. 1.

### 3. Establishing optimal macroscopic properties

The previous section shows examples of several key macroscopic fiber properties listed across the top of Table 1. This section addresses a semi-empirical process for establishing 'optimal'  $\langle OD \rangle$  and  $\langle ID \rangle$  using the parameters listed along the left side of Table 1. The complications in developing a practical theoretical model of the dry-jet wet spinning process are discussed elsewhere [12].

#### 3.1. Average outside diameter, $\langle OD \rangle$

The primary process variables establishing fiber  $\langle OD \rangle$  are spinneret geometry, dope extrusion rate, and take-up velocity. Other second-order process variables influence  $\langle OD \rangle$  such as fiber shrinkage, which depends primarily on vitrification kinetics. These additional second-order variables are not discussed.

##### 3.1.1. Spinneret geometry

The art of designing hollow fiber spinnerets has evolved over several decades. Nevertheless, most of the knowledge is poorly documented and remains proprietary. Factors influencing spinneret design include the requirement of axisymmetric dope flow, control of molecular orientation and elastic-based instabilities, etc. Limitations in fabrication techniques for the bore fluid orifice capillary constrain hollow fiber spinneret design. These limitations are further complicated by the need to supply bore fluid to this capillary in the center of the developing dope flow without disturbing axisymmetric flow upon

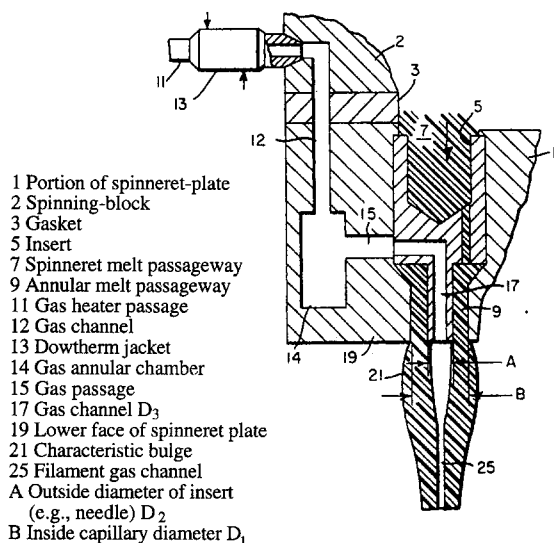


Fig. 8. Reproduction of a patented hollow fiber spinneret cross-section [20] emphasizing the complexity in practical spinneret design. Additional numbers (e.g., 22–24) correspond to other figures in the patent. Note, this spinneret uses a gaseous bore fluid.

leaving the spinneret. The complexity of a practical hollow fiber spinneret design is shown in Fig. 8.

Designing multi-filament spinnerets becomes even more complex and expensive since either numerous individual gear pumps must supply individual capillaries or elaborate hydrodynamic splitting must be completed. These complications justify increasing productivity by maximizing the volumetric extrusion rate through each single capillary. The maximum volumetric dope extrusion rate for a monofilament spinneret is typically limited by the onset of elastic instabilities ranging from die-swell to effects analogous to melt fracture. To minimize elastic effects the length of the rate limiting constriction for dope flow in the spinneret can be increased. However, high pressure drops (many hundred or even thousands of psi) limit this approach.

Orifices for solid filaments even as small as 0.1 mm can be drilled or fabricated using electron discharge machining techniques (EDM) [13]. However, difficulties in fabricating straight capillaries have limited the depth-to-diameter ratios possible by EDM to approximate values of 10:1 restricting small EDM bore capillaries (i.e., < 0.2 mm) to lengths that are too short (i.e., > 2 mm) for practical hollow fiber

spinnerets. Thus, bore fluid capillaries are often drilled or constructed using hypodermic needles. Available needle tolerances limit practical spinneret diameters to about  $D_1 = 0.9$  mm,  $D_2 = 0.4$  mm, and  $D_3 = 0.2$  mm (see Table 1 and Fig. 8). As a result, filaments must be drawn to establish small diameter hollow fibers.

### 3.1.2. Draw ratio

With the spinneret geometry fixed, the primary variable controlling fiber  $\langle OD \rangle$  is the ratio of the average dope extrusion velocity,  $\langle V_i \rangle$ , and take-up velocity,  $V_f$ . This parameter is commonly called the draw ratio or spin-stretch ratio and is defined as:

$$\text{Draw ratio} \equiv \frac{V_f}{\langle V_i \rangle} = \frac{V_f \Pi (D_1^2 - D_2^2)}{4Q_d} \quad (1)$$

where  $Q_d$  is the volumetric dope extrusion rate.  $D_1$  and  $D_2$  define the dope annular cross-section leaving the spinneret. The take-up velocity is established by the speed of a take-up drum or godet. In most small-scale laboratory systems a take-up drum is used. Typical ranges for  $Q_d$  in this study were from 100 to 200 cc/h. The maximum take-up velocity used in this work was 100 m/min.

Increasing the draw ratio decreases  $\langle OD \rangle$  as long as fiber breaks or other complications can be avoided. In dry-jet wet spinning the majority of the drawing occurs in the air gap prior to contacting the quench bath. The rate of tensile strain in the air gap increases with take-up velocity and decreases with extrusion velocity and gap height. Increasing the rate of tensile strain in the air gap tends to increase molecular orientation and fiber breaks.

### 3.2. Average inside diameter, $\langle ID \rangle$

Bore fluids establish and maintain a desired  $\langle ID \rangle$ . The use of many different bore fluids has been reported in the literature [5,14–16]. Our group has explored the use of aqueous salt solutions and solvent–water solutions. Based on our experience, we have rejected salt bore fluids due to their high corrosive tendency. Gaseous bore fluids were not used in this study due to difficulty in controlling the low gas pressure and concern over the ability to prevent oval bores due to reduced vitrification rates.

The influence of the bore fluid is not limited to the establishment of an acceptable lumen shape. The bore fluid undoubtedly alters morphology near the fiber  $\langle ID \rangle$  and permeation properties of the hollow fiber. With the bore fluid composition fixed, remaining spinning parameters are then typically used to adjust permeation properties.

In this study, the typical range of bore fluid rates is from 20 to 70 cc/h. The composition of the bore fluid in this study was typically 90 wt% NMP or DMAC in water. As discussed in the following section, the bore fluid composition was varied as needed to eliminate oval fibers and irregular bores.

#### 4. Complications in establishing optimal macroscopic properties

Initial efforts to establish optimal macroscopic properties may encounter numerous complications. Reaching rigorous conclusions regarding these complications is challenging due to limitations in theoretical modeling of dry-jet wet spinning [12]. The complications discussed here include fiber breaks, diameter variance, irregular fiber shapes, and fiber tension on the drum.

##### 4.1. Fiber breaks

A simple physical visualization of fiber breaks is related to the tensile stress–strain behavior of a solid object such as a rod. Using this description, fiber breaks occur if the *local* tensile stress (i.e., tensile force/fiber cross-sectional area) at some point in the spin line exceeds the local ‘tensile strength’ (i.e., tensile stress at which the fiber breaks). To be quantitatively useful, a means of independently measuring ‘tensile strength’ would be valuable, but performing such rigorous measurements on viscoelastic fluids is typically at least as complicated as practical fiber spinning systems. Therefore, practical experience and correlations between the processing parameters in Table 1 and dope compositional variables like polymer concentration, molecular weight, and solvent quality must currently be relied upon to find stable operating windows with negligible fiber breaks.

Other processing factors besides macroscopic dope compositions are known to influence apparent ‘tensile

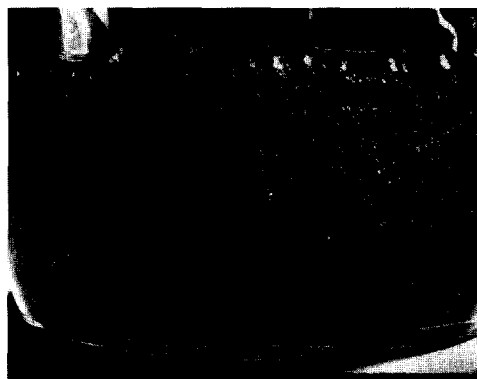


Fig. 9. Photograph of a typical polymeric dope to show ‘bubbles.’ Dope zero shear viscosity is nearly 2000 P.

strength’ of spin lines. For example, dope mixing conditions (i.e., shear intensity and duration), the presence of gas ‘bubbles,’ and time-dependent physical changes in the dope (i.e., dope aging) can limit the ability to form consistent fibers from two apparently identical solutions. Perhaps surprisingly, the mixing of spinning dope components into a homogeneous solution is not a trivial task. The mixing process can take several hours and the entrapment of gas ‘bubbles’ often results (see Fig. 9). Failure to eliminate these gas bubbles prior to spinning can lead to fiber breaks and altered permeation properties.

Moreover, *aging* of dopes may cause differences in properties of spin lines formed from nominally identical dopes differing only in their ‘age’ since the mixing process has been completed. Even when no apparent degradation in polymer molecular weight occurs, complexation and subtle ordering in solutions may alter the rheology of the spin line, tending to result in more spin line breaks. Some dopes in this work that were initially very spinnable were prone to fiber breaks after allowing the dope to age several days or weeks near room temperature. This observation does not appear to be due to changes in overall dope composition. Although such dopes may remain optically transparent, they are apparently not at thermodynamic equilibrium. This observation is supported by Ziabicki who has shown that relaxation spectrums shift as dopes age [17].

For a given spinning dope, these time-dependent changes can be accommodated by altering spinning

conditions to reduce tensile stress and hence fiber breaks. Reducing the draw ratio tends to reduce fiber breaks by decreasing the rate of strain and tensile stress in the air gap during drawing. The draw ratio at which the spin line breaks is often defined as the *critical draw ratio*. Increasing gap height also tends to reduce the rate of strain; however, the effect of gap height on fiber breaks is complicated by hydrodynamic perturbations mentioned later.

In the quench bath, frictional drag from the surrounding fluid and the spin line guides is an additional external force increasing spin line tensile stress and hence fiber breaks in or after the quench bath. Spin line guide friction tends to be more significant than friction with the surrounding fluid and is dependent on the guide surface and the contact angle between the fiber and guide.

#### 4.2. Diameter variations

In the previous description of fiber breaks, the cross-sectional area of the spin line was assumed to be independent of time at any axial position along the spin line. In reality, disturbances in spinning parameters (i.e., flow rates, take-up speed, etc.) can cause time-dependent perturbations in fiber  $\langle OD \rangle$ . The utility of theoretical stability studies related to this complex topic is rather limited [12].

In our work, dope composition and gap height were experimentally found to dramatically affect  $\langle OD \rangle$  variability. Increasing polymer concentration or adding complexing agents such as inorganic salts tended to dampen fiber  $\langle OD \rangle$  variability. These variables, however, tend to affect dope aging mentioned earlier, so careful adjustment is needed. The effect of gap height is even more complex. For a given  $\langle V_i \rangle$  and  $V_f$ , decreasing gap height reduces the time available for perturbation growth prior to vitrification. However, dope flow is strain rate dependent, so the dependence of hydrodynamic perturbation growth on gap height is extremely dope specific. Experimental cases where  $\langle OD \rangle$  variability was reduced by *increasing* gap height were seen almost as frequently as those where it was reduced by *decreasing* gap height. This observation emphasizes that gap height, while a useful variable to assist in achieving spinnability, must be adjusted carefully and with cross-checks on  $\langle OD \rangle$  variability. Fig. 10 shows an

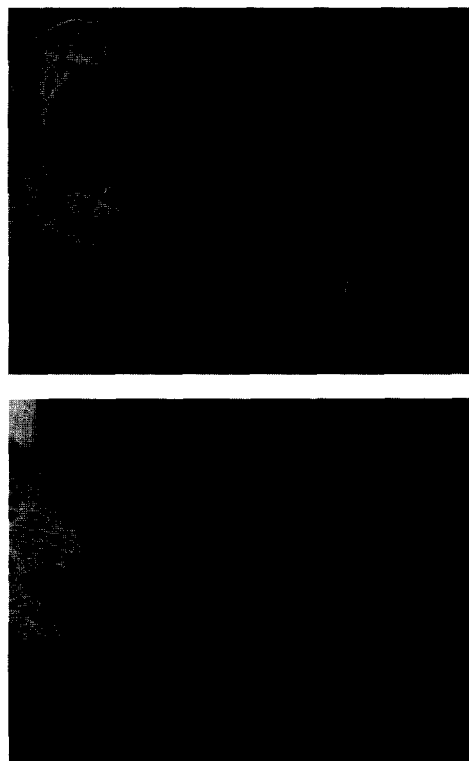


Fig. 10. Scanning electron photomicrographs depicting an example of the possible fiber  $\langle OD \rangle$  variability and its dependence on gap height. Gap height 2.5 cm (top) and 26.5 cm (bottom).

example of the possible fiber  $\langle OD \rangle$  variability and its dependence on gap height.

#### 4.3. Irregular fibers

Nonconcentric bores, irregular bores, and oval fibers are three serious fiber irregularities that must be overcome by establishing acceptable spinning conditions. Nonconcentric bores are sometimes seen during start-up. If they persist, shutting down and recentering the bore fluid capillary will generally be needed to achieve concentricity. Some tolerance in the concentricity of the fiber bore must be accepted, but the ratio of the maximum to minimum wall thickness should not be more than about 1.10 for well-made fibers.

Irregular bores can be eliminated by increasing the solvent concentration in the bore fluid. If the bore fluid contains excessive nonsolvent (e.g., water),



the inside fiber wall begins vitrifying during drawing resulting in an irregular bore as depicted in Fig. 5.

Oval fibers can be eliminated by increasing the residence time in the quench bath prior to contacting the first spin line guide or by increasing the kinetics of vitrification. Complications with ovality occur more frequently with larger fiber diameters (e.g., greater than 300  $\mu\text{m}$ ) due to the prolonged vitrification process limited by mass transfer from the thick fiber wall. Similar problems with oval fibers have been noted by Koops et al. in the preparation of hollow fibers for pervaporation [18]. Use of air in the bore, rather than a nonsolvent liquid, also can cause oval fibers, since only single-sided nonsolvent-solvent removal can occur in this case.

#### 4.4. Fiber tension on take-up drum

A wide range of self-induced axial tension in polysulfone fibers was observed in fibers collected on the final take-up drum. Although generally not a serious enough problem to compromise spinnability, effects ranged from inducing actual fiber breaks to the generation of disorderly fiber windup samples. These problems were never encountered while spinning Ultem® polyetherimide dopes.

Clearly, fiber spun onto a take-up drum versus fiber accelerated by a godet winder experiences a different mechanical environment. Moreover, it seems plausible that these tensile stresses imposed by the take-up device could significantly alter the permeation properties. These differences may contribute to inconsistencies in the permeation performance of fibers spun under conditions naively believed to be identical.

## 5. Summary

This paper is summarized by reconsidering Table 1. Fiber properties identified in the first section of this paper are listed across the top of Table 1 and are categorized as macroscopic properties to distinguish them from other morphological properties crucial in membrane applications. The second section of this paper discusses a practical approach to establishing these properties using the primary processing parameters listed down the left side of Table 1. The last

section identifies several complications often encountered when attempting to establish these properties and provides guidance in overcoming these complications. If optimal macroscopic properties cannot be reliably generated, the utility of a given dope is seriously limited.

## Acknowledgements

Richard Ubersax from Dupont is thanked for his thoughtful comments in preparing this paper. Steve Pesek from Air Liquide is duly noted for his valuable contributions and George Vassilatos and Max Ekiner from Dupont for their critical comments. Sandra Aranyos, Greg Davis, and Karen Shaw are recognized for indirect contributions from their undergraduate research project. The authors are also grateful for the technical and financial contributions of Air Liquide and the E.I. du Pont de Nemours Company.

## Appendix A. Establishing macroscopic properties – A case study

### A.1. Objective

To spin a polysulfone hollow fiber with  $\langle\text{OD}\rangle/\langle\text{ID}\rangle = 2$  and outside diameter of 200  $\mu\text{m}$  from a dope containing a volatile solvent with a relatively large air gap (i.e.,  $> 15\text{ cm}$ ) so the effects of mass transfer in the air gap can be investigated.

### A.2. Background

Previously, Pesek measured very attractive permeation properties, even without post-treatment, for polysulfone hollow fibers he spun from a dope composed of 40 wt% polysulfone (Udel® 1800), 36 wt% DMAC, 12 wt% THF, and 12 wt% EtOH [19]. However, he did not focus on developing optimal macroscopic properties as a cross-section of the fiber illustrates in Fig. 5.

### A.3. Procedure

To reduce fiber  $\langle\text{OD}\rangle$  from over 500  $\mu\text{m}$  to about 200  $\mu\text{m}$  the draw ratio was increased from 2.1 to 10

primarily by increasing the take-up speed,  $V_f$ , to 80 m/min. Unfortunately, spin line continuity could not be maintained and frequent breaks occurred, suggesting the 'tensile strength' was exceeded. Without drastically altering the thermodynamic nature of Pesek's dope, the only plausible means of increasing the apparent 'tensile strength' was to increase the molecular weight of the polysulfone to the highest commercially available (Udel® 1835).

Fibers spun from Udel® 1835 at a draw ratio of 10 using 85 wt% aqueous DMAC bore solution continually produced optimal macroscopic properties when the gap height was less than 10 cm (see Fig. 1). At gap heights greater than about 10 cm,  $\langle OD \rangle$  variability was excessive requiring dope reformation to meet the long term objective (i.e., spinning stability with gap heights > 10 cm).

As discussed in this paper, increasing dope viscosity tends to dampen fiber diameter variability. Polymer concentration and the choice of solvent-nonsolvent pairs do alter viscosity; however, these effects are second order to the effect of complexing agents such as lithium nitrate.

As a result of adding lithium nitrate, the spinneret temperature had to be raised to reduce excessive pressure drops across the spinneret (e.g., > 2000 psid) compromising isothermal processing conditions near room temperature. Elevated processing temperatures also required substituting THF (boiling point 65–67°C) with 1,4-dioxane (b.p. 100–102°C) and EtOH (b.p. 78–79°C) with isobutanol (b.p. 99–100°C) at the expense of the decreased miscibility of isobutanol with water. With these new components established, miscibility limits were determined by increasing nonsolvent concentration. A *stable*, suitable dope composition was identified as 37.5% PSF (Udel® 1835), 42.3% NMP, 14.1% 1,4-dioxane, 4.7% isobutanol, and 1.4% lithium nitrate.

With this dope, optimal fiber properties, similar to those shown in Fig. 1, could be obtained over a wider range of gap heights.

## References

- [1] H.I. Mahon, Permeability separatory apparatus and membrane element, method of making the same and process utilizing the same, U.S. Patent 3,228,876, Dow Chemical, 1966.
- [2] H.I. Mahon, Permeability separator apparatus and process using hollow fibers, U.S. Patent 3,228,877, Dow Chemical, 1966.
- [3] O.M. Ekiner and G. Vassilatos, Polymeric membranes, U.S. Patent 5,102,600, E.I. du Pont de Nemours and Co., 1992.
- [4] S. Loeb and S. Sourirajan, High flow porous membranes for separating water from saline solutions, U.S. Patent 3,133,132, 1964.
- [5] I. Cabasso, E. Klein and J.K. Smith, Polysulfone hollow fibers. I. Spinning and properties, *J. Appl. Polym. Sci.*, 20 (1976) 2377–2394.
- [6] I. Cabasso, E. Klein and J.K. Smith, Polysulfone hollow fibers. II. Morphology, *J. Appl. Pol. Sci.*, 21 (1977) 165–180.
- [7] R.E. Kesting, *Synthetic Polymeric Membranes*, McGraw-Hill, New York, 1971.
- [8] H. Strathmann, P. Scheible and R.W. Baker, A rationale for the preparation of Loeb–Sourirajan-type cellulose acetate membranes, *J. Appl. Polym. Sci.*, 15 (1971) 811–828.
- [9] H. Strathmann et al., The formation mechanism of asymmetric membranes, *Desalination*, 16 (1975) 179–203.
- [10] C.A. Smolders et al., Microstructure in phase-inversion membranes. Part 1. Formation of macrovoids, *J. Membr. Sci.*, 73 (1992) 259–275.
- [11] O.M. Ekiner and G. Vassilatos, Polyaramide hollow fiber for hydrogen/methane separation-spinning and properties, *J. Membr. Sci.*, 53 (1990) 259–273.
- [12] S.A. McKelvey, Formation and Characterization of Asymmetric Hollow Fiber Membranes for Gas Separation Applications, Ph.D. Thesis, University of Texas at Austin, 1996, tentatively.
- [13] J. Sebzda, Small hole EDM review, *EDM Today*, March/April (1996) 35–37.
- [14] S.-G. Li et al., Wet spinning of integrally skinned hollow fiber membranes by a modified dual-bath coagulation method using a triple orifice spinneret, *J. Membr. Sci.*, 94 (1994) 329–340.
- [15] S.C. Pesek, Aqueous Quenched Asymmetric Polysulfone Flat Sheet and Hollow Fiber Membranes Prepared by Dry/Wet Phase Separation, Ph.D. Thesis, University of Texas at Austin, 1993.
- [16] J. van't Hof, Wet Spinning of Asymmetric Hollow Fibre Membranes for Gas Separation, Ph.D. Thesis, Universiteit Twente, The Netherlands, 1988.
- [17] A. Ziabicki, *Fundamentals of Fiber Formation*, Wiley, New York, 1976.
- [18] G.H. Koops et al., Integrally skinned polysulfone hollow fiber membranes for pervaporation, *J. Appl. Polym. Sci.*, 54 (1994) 385–404.
- [19] S.C. Pesek and W.J. Koros, Aqueous quenched asymmetric polysulfone hollow fibers prepared by dry/wet phase separation, *J. Membr. Sci.*, 88 (1994) 1–19.
- [20] R.Y. Hayes, Method and apparatus for melt-spinning hollow fibers, U.S. Patent 3,686,377, E.I. du Pont de Nemours and Co., 1971.